Scientific Research Publishing

Journal of Modern Physics, 2023, 14, 101-110
https://www.scirp.org/journal/jmp
ISSN Online: 2153-120X
ISSN Print: 2153-1196

Highly Efficient Two-Channel Drop Filter of Single Photons with One Drop Waveguide

Jinsong Huang, Ximeng Feng

School of Information Engineering, Jiangxi University of Science and Technology, Ganzhou, China
Email: jshuangjs@126.com

How to cite this paper: Huang, J.S. and Feng, X.M. (2023) Highly Efficient Two-Channel Drop Filter of Single Photons with One Drop Waveguide. *Journal of Modern Physics*, **14**, 101-110.
https://doi.org/10.4236/jmp.2023.142007

Received: December 8, 2022
Accepted: January 16, 2023
Published: January 19, 2023

Abstract

A novel double-channel drop filter of single photons with only a drop waveguide is proposed. In the structure, two microresonators with a qubit are used to connect the drop waveguide and the bus waveguide with a reflector. By tuning the system parameters, multiple wavelengths with high drop efficiencies in two output channels of the drop waveguide are obtained. As the reflector is independent on its exact location, and one drop waveguide with two drop channels saves the integrated space, this may suggest a potential filtering device which functions in photonic integrated circuits and dense wavelength division multiplexing communication.

Keywords

Optical Filter, Scattering Theory, Optical Waveguide, Microresonator

1. Introduction

Optical drop filters are the essential elements in photonic integrated circuits and dense wavelength division multiplexing (WDM) communication systems, since they have been applied as multiplexers, selector, modulators, and so on. Over the past two decades, a variety of investigation on optical drop filtering has been carried out in various systems, including fiber Bragg gratings [1]-[6], photonic crystal structures [7]-[17], plasmonic systems [18] [19], and microresonators [20]-[25], etc. Especially, whispering-gallery mode (WGM) resonators as filter components have attracted much attention owing to their high quality factors and compact sizes [26]. With such a filter coupled with a single-mode resonator, the desired wavelength with high efficiency is selected to drop in one output channel of the drop waveguide, while another output port is free, as the single-mode direction does not match the transmission direction in the free port.

As an extension of single channel filters, multi-channel filtering has drawn wide concern, since multiple signals can be dropped to meet the demands of multiplexing. Usually, numerous filters based on single coupled resonators were designed to implement single resonance wavelength outputs within each drop waveguide channel. It should be interesting to perform two-channel filtering by only one drop waveguide, when only drop function is considered in two ports. Using the free port increases the drop channel capacity with different wavelengths, and reduces the complexity of the structure, which saves the integrated space of the coupled filtering device.

Inspired by these considerations, we extend the single coupled-resonator configuration [20] and propose a two-channel filter with a drop waveguide, which are side-coupled to two resonators with a qubit. A reflector requiring no exact location is utilized to reflect the photons to investigate how to perform two-channel filtering of single photons with high drop efficiency. By employing a real-space Hamiltonian, the photon scattering amplitudes in two output ports of the drop waveguide are obtained theoretically. Our results show that multiple peak wavelengths in the two-channel structure with high drop efficiencies can be achieved, by adjusting the waveguide-resonator and qubit-resonator coupling strengths. Hence, the proposed compact filtering systems provide potential applications in photonic integrated circuits and dense WDM networks.

2. Theoretical Model

As shown in Figure 1, a two-channel filtering system is formed by a bus waveguide and a drop waveguide, and these two waveguides are connected by two

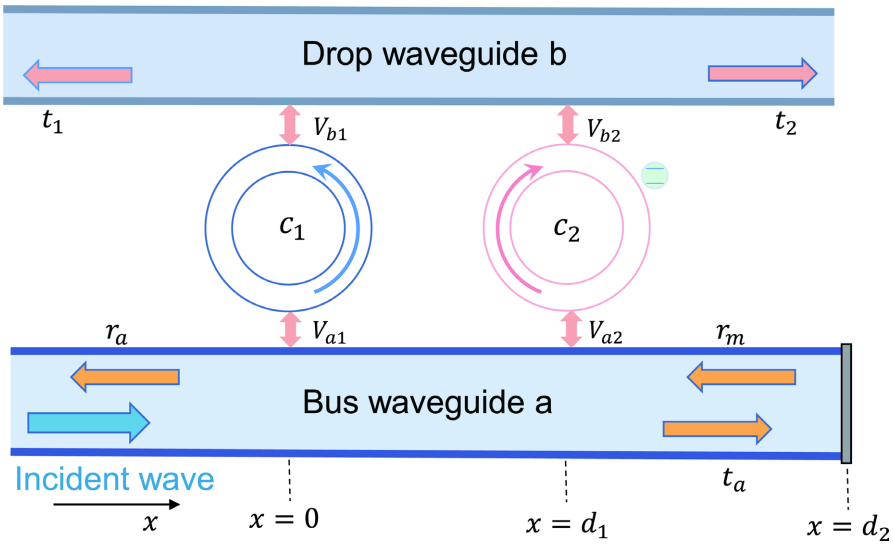

Figure 1. (Color online) Schematic diagram for a drop filter of single photons constructed by two waveguides coupled to two single-mode whispering gallery resonators. The second resonator is also coupled to a two-level system (qubit). A perfect mirror is used to reflect the photons in the bus waveguide to transmit along the right port in the drop waveguide. The incident photon from the left port of the bus waveguide is reflected, or dropped to the two ports of the drop waveguide by two coupled resonators.

single-mode whispering gallery resonators separated by a distance d_1. The two resonators hold two inversus rotary modes, described by the creation operator $c_n^\dagger$ ($n=1,2$ throughout the paper), with the resonance frequency ω_{cn}. The second resonator is also coupled to a two two-level system (qubit) characterized by the ground state $|g\rangle$ and excited state $|e\rangle$, with the coupling strength ξ. When a single photon is input from the left side of the bus waveguide, it is coupled to the resonator-1 at $x=0$, and dropped to the left port of the waveguide-b. To increase the drop channel number, a perfect reflecting mirror located at $x=d_2$ is utilized to redirect the photons to couple another resonator-2, owing to direction matching of the resonator and guided-wave modes, and then transfer the photons to the right port of the drop waveguide. As seen in Figure 1, the right port of the drop waveguide is also employed to save the device area, and a two-channel drop filter with only one drop waveguide is constructed effectively.

The real-space Hamiltonian [27] for the filtering system can be expressed as ($\hbar=1$)

$$\begin{aligned} H=&\sum_{m=a,b}\int \mathrm{d}x\left[-i\upsilon_g C_{Rm}^\dagger(x)\frac{\partial}{\partial x}C_{Rm}(x)+i\upsilon_g C_{Lm}^\dagger(x)\frac{\partial}{\partial x}C_{Lm}(x)\right]\\ &+\sum_{n=1,2}(\omega_{cn}-i\gamma_{cn})c_n^\dagger c_n+(\omega_e-i\gamma_e)\sigma_+\sigma_-+\xi\left(c_2^\dagger\sigma_-+c_2\sigma_+\right)\\ &+\int \mathrm{d}x\delta(x)\left\{V_{a1}\left[C_{Ra}^\dagger(x)c_1+H.c.\right]+V_{b1}\left[C_{Lb}^\dagger(x)c_1+H.c.\right]\right\}\\ &+\int \mathrm{d}x\delta(x-d_1)\left\{V_{a2}\left[C_{La}^\dagger(x)c_2+H.c.\right]+V_{b2}\left[C_{Rb}^\dagger(x)c_2+H.c.\right]\right\}. \end{aligned} \quad (1)$$

Here, we have taken the ground-state level of the qubit as the energy reference. $C_{Rm}^\dagger(x)$ $\left[C_{Lm}^\dagger(x)\right]$ represents the generation of a right-travelling (left-travelling) photon at x in the waveguide-m, and υ_g is the group velocity of the photon propagation. $\delta(x)\left[\delta(x-d_1)\right]$ indicates that the resonator-waveguide interaction occurs at $x=0(d_1)$. $\sigma_+=|e\rangle\langle g|$ and $\sigma_-=|g\rangle\langle e|$ denote the raising and lowering operators of the qubit with a transition frequency ω_e, respectively. V_{mn} describes the coupling strength between the resonator-n and the waveguide-m, and γ_{cn} and γ_e stand for the energy loss rates for the resonators and qubits, respectively.

Assume that a single photon is incident from the left port of the bus waveguide with the energy $E_k=\upsilon_g k=\omega$. The scattering eigenstate of the Hamiltonian (1) is written as

$$|\varphi\rangle=\sum_{m=a,b}\int \mathrm{d}x\left[\phi_{Rm}(x)C_{Rm}^\dagger(x)+\phi_{Lm}(x)C_{Lm}^\dagger(x)\right]|\varnothing\rangle+\sum_{n=1,2}\left(\eta_n c_n^\dagger+\zeta\sigma_+\right)|\varnothing\rangle. \quad (2)$$

$\phi_{Rm}(x)$ and $\phi_{Lm}(x)$ represent the single-photon wave functions along the right and left directions in the waveguide-m. $|\varnothing\rangle=|0_a,0_b,0_1,0_2,g\rangle$ describes the vacuum states of waveguides and resonators and the ground state of the qubit. η_n and ζ are the excitation amplitudes of the resonator modes and excited state of the qubit, respectively.

The corresponding wave functions take the forms

$$\begin{aligned}
&\phi_{Ra}(x) = \mathrm{e}^{ikx}\left[\theta(-x) + t_a\theta(x)\right],\\
&\phi_{La}(x) = \mathrm{e}^{-ikx}\left[r_a\theta(d_1 - x) + r_m\theta(x - d_1)\right],\\
&\phi_{Rb}(x) = \mathrm{e}^{ikx}t_2\theta(x - d_1),\\
&\phi_{Lb}(x) = \mathrm{e}^{-ikx}t_1\theta(-x),
\end{aligned} \tag{3}$$

where, t_1 and t_2 represent the transmission amplitudes for two ports in the drop waveguide, and t_a and r_a represent the transmission and reflection amplitudes in the bus waveguide, respectively. r_m is the reflection amplitude from the reflector. $\theta(x)$ is the Heaviside step function, with $\theta(0) = 1/2$.

By solving the eigen-equation $H|\psi\rangle = E_k|\psi\rangle$ with the boundary condition $\phi_{Ra}(d_2) + \phi_{La}(d_2) = 0$ at the bus waveguide, one can obtain the expressions of these scattering amplitudes

$$\begin{aligned}
t_1 &= -\frac{i\sqrt{\Gamma_{a1}\Gamma_{b1}}}{Q_1},\\
t_2 &= \mathrm{e}^{2i(\phi_2-\phi_1)}\frac{i\sqrt{\Gamma_{a2}\Gamma_{b2}}N}{Q_2N - \xi^2}\left(\frac{i\Gamma_{a1}}{Q_1} - 1\right),\\
t_a &= 1 - \frac{i\Gamma_{a1}}{Q_1},\\
r_a &= \mathrm{e}^{2i\phi_2}\left[1 - \frac{i\Gamma_{a2}N}{Q_2N - \xi^2}\right]\left(\frac{i\Gamma_{a1}}{Q_1} - 1\right).
\end{aligned} \tag{4}$$

Here, $Q_1 = \Delta\omega + i\gamma_{c1} + i(\Gamma_{a1} + \Gamma_{b1})/2$, $Q_2 = \Delta\omega + \Delta\omega_{12} + i\gamma_{c2} + i(\Gamma_{a2} + \Gamma_{b2})/2$, $N = \Delta\omega + \Delta\omega_e + i\gamma_e$. In general, the frequencies of two resonator modes and the atomic transition frequency may be different, thus we introduce these detunings, where $\Delta\omega = \omega - \omega_{c1}$ is the frequency detuning between the incident wave and the resonator-1, $\Delta\omega_{12} = \omega_{c1} - \omega_{c2}$ is the frequency detuning from two resonators, and $\Delta\omega_e = \omega_{c1} - \omega_e$ is the frequency detuning between the resonator-1 and the coupled qubit. $\Gamma_{an} = V_{an}^2/\upsilon_g$, $\Gamma_{bn} = V_{bn}^2/\upsilon_g$, $\phi_n = kd_n$, with $n = 1, 2$.

3. Single-Photon Filtering in the Coupled Waveguide System

For the two-channel structure, the filtering properties of single photons are characterized by these transmission $T_{a(1,2)} = |t_{a(1,2)}|^2$ and reflection $R_a = |r_a|^2$. As a review, we first consider the case that there is no reflector at the right end of the bus waveguide. When a single photon enters from the left port of the bus waveguide, it will propagate from left to right along the bus waveguide, or transfers to the left side of the drop waveguide with the help of the coupled single-mode resonator-1, while it cannot be redirected to the right port of the drop waveguide, due to the mode-direction matching condition from the resonator and guided-wave modes.

Figure 2(a) shows the photon transmission versus the frequency detuning $\Delta\omega$ in two waveguides. As seen, the photon-flow conservation $T_a + T_1 = 1$ (see the yellow straight line) for all frequencies is satisfied when the dissipations are

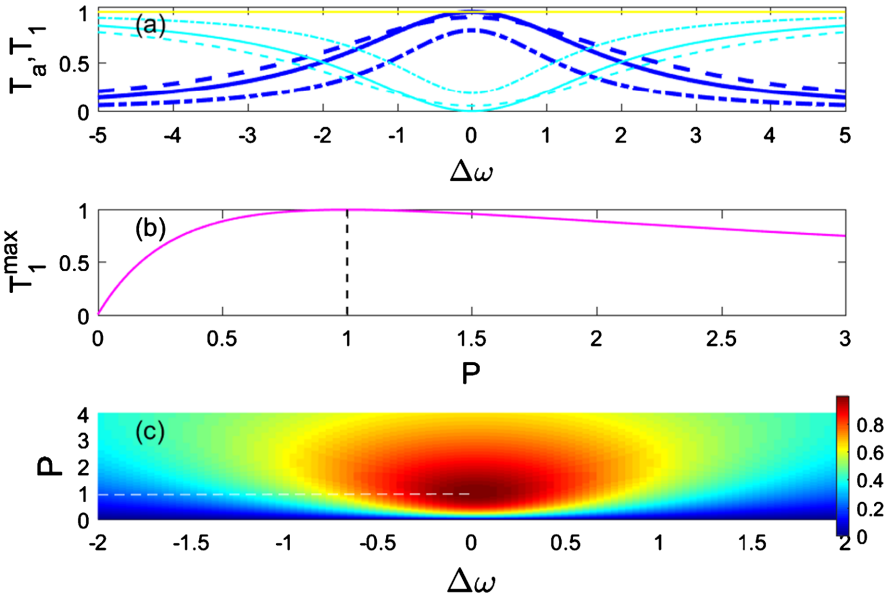

Figure 2. (Color online) (a) The transmission T_a (thin cyan lines) and the drop efficiency T_1 (thick blue lines) versus different coupling ratios: $P=0.4$ (dashed curves), $P=1$ (solid curves), and $P=1.6$ (dash dotted curves). (b) The maximum drop efficiency $T_1^{\max}$ versus the coupling ratio P. (c) T_1 as a function of coupling ratio P and $\Delta\omega$. Zero dissipation ($\gamma_{c1}=0$) is set. For convenience, all the parameters are in units of Γ_{a1}.

excluded. In addition, single drop peak for T_1 with maximum drop efficiency of unity is exhibited at resonance $\Delta\omega=0$ when the coupling ratio $P=\Gamma_{b1}/\Gamma_{a1}=1$. This implies that the traveling photon along the bus waveguide is totally blocked by the first resonator, and then routed to the drop waveguide, as demonstrated in Ref. [20]. To further investigate the dependence of the filtering efficiency on the coupling ratio P, we plot their relationship in **Figure 2(b)** and **Figure 2(c)**. It can be observed that only when two resonator-waveguide coupling Γ_{b1} and Γ_{a1} are equal, T_1 can reach the maximum drop efficiency of 1 or present a dark red peak with the maximum value. Since a symmetrical transmission path through two waveguides is generated under this condition, the incident photons can transfer completely between two waveguides.

When the reflecting mirror is included, another output channel emerges, as travelling photons are reflected and coupled to the second whispering gallery resonator with an opposite rotation mode, and then routed into the right drop port. As a contrast, we consider the bare resonator case, in which the second resonator and the qubit are decoupled and their coupling strength ξ is assumed to be zero. The optical field distributions in two drop channels for the detuning $\Delta\omega$ are depicted in **Figure 3**. Note that the drop transmission T_2 in the right drop channel results from these off-resonant signals via the reflection of the perfect mirror, and thus the drop peak of T_1 in the left drop channel will always remain unchanged at the resonance point. As shown in **Figure 3(a)**, zero transmission for T_2 appears at the resonance point, and two minimum peaks of T_2 (dashed curves) are presented for the zero inter-resonator detuning ($\Delta\omega_{12}=0$),

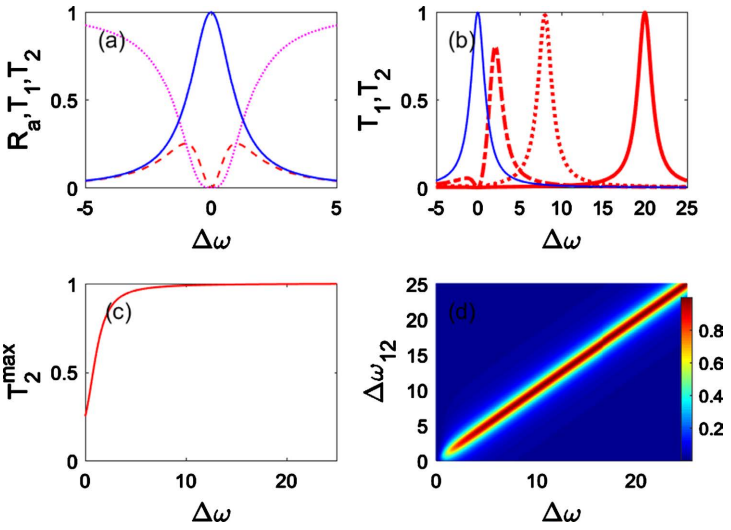

Figure 3. (Color online) (a) The drop transmission T_1 (blue solid line) and T_2 (dashed line), and the reflection R_a (magenta dotted line) for zero inter-resonator detuning $\Delta\omega_{12}=0$. (b) T_1 (blue thin line) and T_2 (red thick line) for different inter-resonator detuning: $\Delta\omega_{12}=2,8,20$ (dotted line, dash dotted line, solid line). (c) The maximum drop efficiency $T_2^{\max}$ versus the inter-resonator detuning $\Delta\omega_{12}$. (d) T_2 as a function of $\Delta\omega_{12}$ and $\Delta\omega$. Other parameters are set as: $\Gamma_{b1}=\Gamma_{a2}=\Gamma_{b2}=1$, $\gamma_{c1}=\gamma_{c2}=0$.

arising from the strongest interference of two drop signals.

When increasing the inter-resonator detuning to separate their resonance frequencies, quantum interference and its induced crosstalk of two channel signals are lowered, and thus the drop efficiency of the additional channel is improved. **Figure 3(b)** and **Figure 3(c)** show that the drop peak values of T_2 increase with a frequency shift equal to the inter-resonator detuning when varying the inter-resonator detuning. **Figure 3(d)** further displays that the drop peaks with maximum values of ones are exhibited in a narrow and straight crimson region with a threshold value around $\Delta\omega_{12}=10$. Therefore, it reveals that the signal crosstalk in the two channels can be suppressed by adjusting the detuning between two resonators. Notice that these transmissions are independent of the accurate position of the reflecting mirror in the reflection feedback, which can be found in Equation (4), since the mode-direction matching condition is satisfied by the horizontal reflection direction and rotation mode direction of the resonator. In contrast to the previous schemes requiring the precise phase shifts in connection with the locations [7] [8] [9], the kind of filters have great advantages.

When the qubit is attached to the second resonator, high drop efficiencies can be achieved in another way. As described in **Figure 3(a)**, T_2 is small when $\Delta\omega_{12}=0$ and there is not the coupled qubit ($G=0$). However, as G continues to increase, two peak values of T_2 gradually increase and reach to unities, as displayed in **Figure 4**. Moreover, two separated drop peaks of T_2, located around the resonance point $\Delta\omega=0$ with $\pm G$ (assuming $\omega_e=\omega_1$), are distributed symmetrically due to the Rabi splitting effect. Similar to the above case of tuning inter-resonator detuning, the drop peak of T_1 with the maximum value of 1

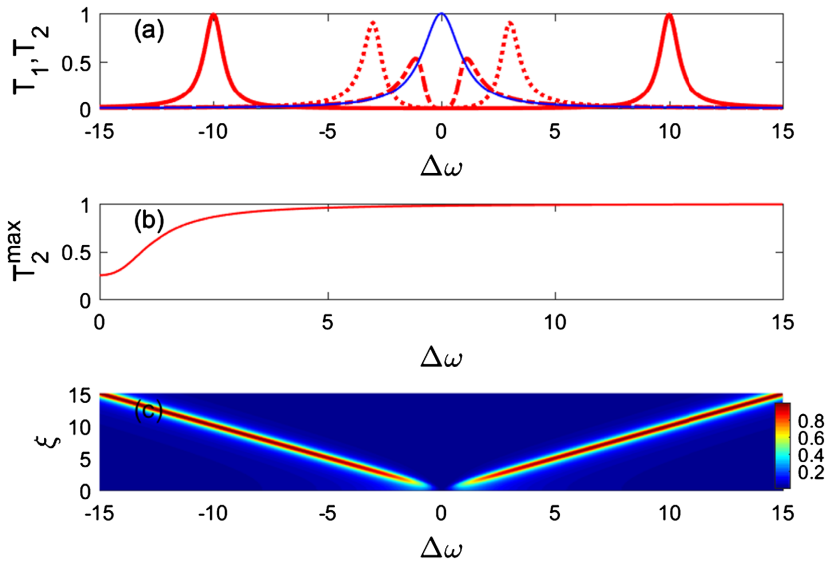

Figure 4. (Color online) (a) The drop transmission T_1 (blue thin line) and T_2 (red thick lines) for different coupling strengths ξ: $g = 1,3,10$ (dash dotted lines, dotted lines, solid lines). (b) $T_2^{\max}$ versus the coupling strength ξ, coupling strength g, (c) T_2 as a function of the coupling strength ξ and $\Delta\omega$. Other parameters are $\Gamma_{b1} = \Gamma_{a2} = \Gamma_{b2} = 1$, $\gamma_{c1} = \gamma_{c2} = \gamma_e = 0$.

remains unchanged at the resonance point $\Delta\omega = 0$, while the drop peak of T_2 expanded in a *V*-shaped area with the frequency shifts related to *G*, and goes slowly up to unity, as shown in **Figure 4(b)** and **Figure 4(c)**. The resonator-qubit coupling strength can be controlled by their separation or the polarization of the atomic exciton. For instance, the coupling is tuned by using an external field to orient the direction of the dipole moment of the atomic exciton [27] [28]. Consequently, controlling the resonator-qubit coupling can also serve as a novel path to perform highly-efficient filtering, because the widen frequency interval generated by the Rabi splitting can suppress the interference from these filtering signals.

To gain a deeper insight into the effect of the resonator-waveguide couplings on the drop efficiencies of two drop ports, **Figure 5** plots the drop spectra for different coupling ratios. For simplification, $P = \Gamma_{b1}/\Gamma_{a1} = \Gamma_{b2}/\Gamma_{a2}$ is here taken as the coupling ratio for two resonator-waveguide couplings. It is shown in **Figure 5(a)** that two drop peaks can synchronously reach the maximum values under the condition $P = 1$ for an inter-resonator detuning $\Delta\omega_{12} = 15$. It indicates that two maximum drop efficiencies of unities can be realized in two frequency locations with a separation of $\Delta\omega_{12}$, since the symmetrical coupling paths through two waveguides results in the complete transfer of these signals, as mentioned previously. Similarly, three drop peaks in two channels emerge for four equal resonator-waveguide couplings, when the qubit is coupled and there is not inter-resonator detuning, as depicted in **Figure 5(b)**. In the case, a white straight line of $P = 1$ also passes through these peak regions.

Note that the dissipations are not taken into account in the above discussions.

In fact, the coupled system inevitably experiences dissipations. In contrast with the ideal case with no dissipations, these drop efficiencies of T_1 and T_2 in the filtering spectra decrease with the increasing dissipations, and two drop frequencies of T_2 experience more leakages with the Rabi-splitting effects, as displayed in Figure 6. For a high-quality microresonator with very low losses, however, high drop efficiency is still available, such as the appropriate result around 0.8 for T_2 when $\gamma = 0.05$.

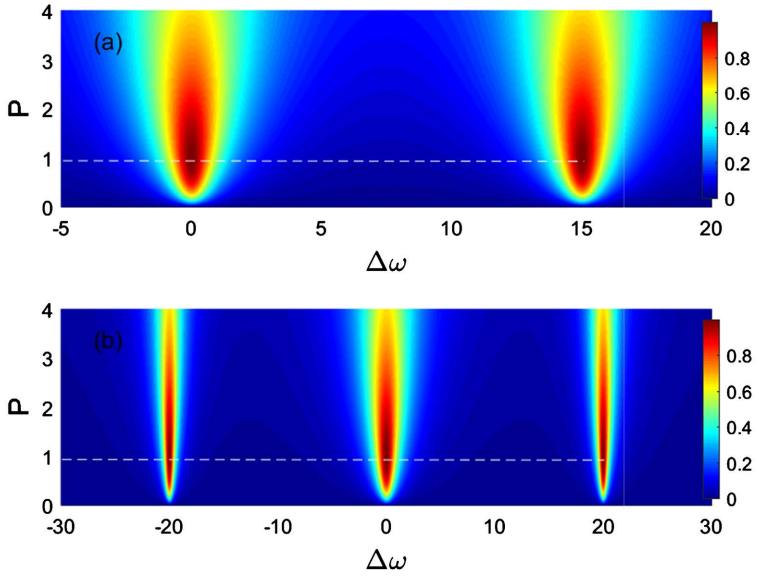

Figure 5. (Color online) T_1 in (a) and T_2 in (b) as a function of the coupling ratio P and $\Delta\omega$. (a) $g = 0$, $\Delta\omega_{12} = 15$. (b) $g = 10$, $\Delta\omega_{12} = 0$. Dissipations are assumed to be zeroes.

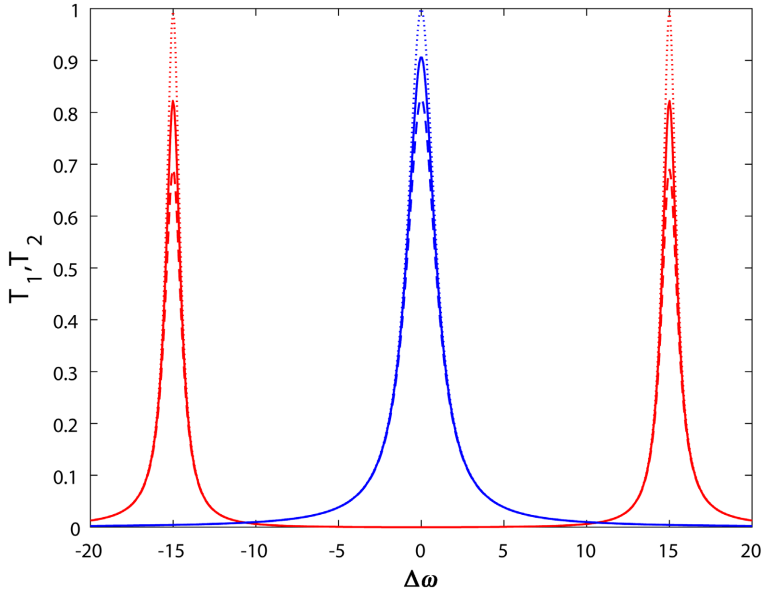

Figure 6. (Color online) T_1 (middle line) and T_2 (left and right lines) for different dissipations: $\gamma = 0, 0.05, 0.1$ (dotted lines, solid lines, dash dotted lines). Other parameters are $P = 1$, $g = 20$, $\Delta\omega_{12} = 0$.

4. Conclusion

In summary, we have proposed a dual-channel quantum filter of single photons with only one drop waveguide, which saves the integrated space of the coupled device. Our results show that double or triple drop peaks with high drop efficiencies can be achieved in the transmission spectra, by adjusting the frequency detuning between two resonators or the resonator-qubit coupling. In addition, the reflection feedback in the system does not require exact location of the reflector, which has advantages over the schemes dependent on the phase shifts related to the locations. As the proposed structure is able to generalize easily to a multiple two-channel one by coupling more drop waveguides, it may have potential in photonic integrated circuits and dense WDM optical communication systems.

Acknowledgments

This work was supported by Natural Science Foundation of Jiangxi Province (Grant No. 20212BAB201014).

Conflicts of Interest

The authors declare no conflicts of interest regarding the publication of this paper.

References

[1] Bilodeau, F., Johnson, D.C., Theriault, S., Malo, B., Albert, J. and Hill, K.O. (1995) *IEEE Photonics Technology Letters*, **7**, 388. https://doi.org/10.1109/68.376811

[2] Riziotis, C. and Zervas, M.N. (2001) *Journal of Lightwave Technology*, **19**, 92-104. https://doi.org/10.1109/50.914490

[3] Hamarsheh, M.M.N., Falah, A.A.S. and Mokhtar, M.R. (2015) *Optical Engineering*, **54**, Article ID: 016105. https://doi.org/10.1117/1.OE.54.1.016105

[4] Yun, B., Hu, G., Zhang, R. and Cui, Y. (2015) *Optics Communications*, **336**, 30-33. https://doi.org/10.1016/j.optcom.2014.09.048

[5] Zhang, Z.X., Mou, C.B., Yan, Z.J, Wang, Y.J., Zhou, K.M. and Zhang, L. (2015) *Optics Express*, **23**, 1353-1360. https://doi.org/10.1364/OE.23.001353

[6] Yang, J.J., Fan, J., Zou, Y.G., Wang, H.Z. and Ma, X.H. (2022) *Chinese Physics B*, **31**, Article ID: 084203. https://doi.org/10.1088/1674-1056/ac5391

[7] Kim, S., Park, I., Lim, H. and Kee, C.S. (2004) *Optics Express*, **12**, 5518. https://doi.org/10.1364/OPEX.12.005518

[8] Ren, H.L., Chun, J., Hu, W.S., Gao, M.Y. and Wang, J.Y. (2006) *Optics Express*, **14**, 2446. https://doi.org/10.1364/OE.14.002446

[9] Ren, H.L., Zhang, J.H., Qin, Y.L., Li, J., Guo, S.Q., Hu, W.S., Jiang, C. and Jin, Y.H. (2013) *Optik*, **124**, 1787-1791. https://doi.org/10.1016/j.ijleo.2012.05.017

[10] Qiang, Z.X., Zhou, W.D. and Soref, R.A. (2007) *Optics Express*, **15**, 1823-1831. https://doi.org/10.1364/OE.15.001823

[11] Monifi, F., Ghaffari, A., Djavid, M. and Abrishamian, M.S. (2003) *Applied Optics*, **48**, 804-809. https://doi.org/10.1364/AO.48.000804

[12] Barati, M. and Aghajamali, A. (2016) *Physica E*, **79**, 20-25. https://doi.org/10.1016/j.physe.2015.12.012

[13] Kumar, A., Suthar, B., Kumar, V., Bhargava, A., Singh, K.S. and Ojha, S.P. (2013) *Optik*, **124**, 2504-2506. https://doi.org/10.1016/j.ijleo.2012.08.030

[14] Wang, H.T., Timofeev, I.V., Chang, K., Zyryanov, V.Y. and Lee, W. (2014) *Optics Express*, **22**, 15097. https://doi.org/10.1364/OE.22.015097

[15] Zhao, X.D., Yang, Y.B., Wen, J.H., Chen, Z.H., Zhang, M.D., Fei, H.M. and Hao, Y.Y. (2017) *Applied Optics*, **56**, 5463. https://doi.org/10.1364/AO.56.005463

[16] Wong, B.M. and Morales, A. M. (2009) *Journal of Physics D: Applied Physics*, **42**, Article ID: 055111. https://doi.org/10.1088/0022-3727/42/5/055111

[17] Li, Z.F., Aydin, K. and Ozbay, E. (2008) *Journal of Physics D: Applied Physics*, **41**, Article ID: 155115. https://doi.org/10.1088/0022-3727/41/15/155115

[18] Khani, S., Danaie, M. and Rezaei, P. (2018) *Optical Engineering*, **57**, Article ID: 107102. https://doi.org/10.1117/1.OE.57.10.107102

[19] Geng, X.M., Wang, T.J., Yang, D.Q., He, L.Y. and Wang, C. (2016) *IEEE Photonics Journal*, **8**, Article ID: 4801908. https://doi.org/10.1109/JPHOT.2016.2573041

[20] Monifi, F., Friedlein, J., Özdemir, S.K. and Yang, L. (2012) *Journal of Lightwave Technology*, **30**, 3306. https://doi.org/10.1109/JLT.2012.2214026

[21] Monifi, F., Özdemir, S.K. and Yang, L. (2013) *Applied Physics Letters*, **103**, Article ID: 181103. https://doi.org/10.1063/1.4827637

[22] Lee, Y.J., Lee, D.E. and Kwon, S.K. (2017) *IEEE Photonics Journal*, **9**, Article ID: 6601607.

[23] Zhou, Z.H., Chen, Y., Shen, Z., Zou, C.L., Guo, G.C. and Dong, C.H. (2018) *IEEE Photonics Journal*, **10**, Article ID: 7101607. https://doi.org/10.1109/JPHOT.2017.2764071

[24] Yin Y.H., Niu, Y.X., Dai, L.L. and Ding, M. (2018) *IEEE Photonics Journal*, **10**, Article ID: 7103810. https://doi.org/10.1109/JPHOT.2018.2849976

[25] Deng, L., Li, D.Z., Liu, Z.L., Meng, Y.H., Guo, X.N. and Tian, Y.H. (2017) *Chinese Physics B*, **26**, Article ID: 024209. https://doi.org/10.1088/1674-1056/26/2/024209

[26] Vahala, K.J. (2003) *Nature*, **424**, 839-846. https://doi.org/10.1038/nature01939

[27] Shen, J.T. and Fan, S.H. (2009) *Physical Review A*, **79**, Article ID: 023838. https://doi.org/10.1103/PhysRevA.79.039904

[28] Srinivasan, K. and Painter, O. (2007) *Physical Review A*, **75**, Article ID: 023814. https://doi.org/10.1103/PhysRevA.75.023814